Modeling of Plasma Response to RMP Fields in MAST and ITER

Yueqiang Liu 1), B.D. Dudson 2), Y. Gribov 3), M.P. Gryaznevich 1), T.C. Hender 1), A. Kirk 1), E. Nardon 4), M.V. Umansky 5), H.R. Wilson 2) and X.Q. Xu 5)

1)Euratom/CCFE Fusion Association, Culham Science Centre, Abingdon, OX14 3DB, UK
2)Department of Physics, University of York, Heslington, York YO10 5DD, UK
3) ITER Organization, Route de Vinon sur Verdon, 13115 St Paul Lez Durance, France
4) Euratom/CEA Fusion Association, 13108 St Paul-lez-Durance, France
5) Lawrence Livermore National Laboratory, Livermore, CA 94551, USA

E-mail contact of the main author: yueqiang.liu@ccfe.ac.uk

Abstract. The resonant magnetic perturbation (RMP) fields, including the plasma response, are computed within a linear, full toroidal, single-fluid resistive MHD model. Under realistic plasma conditions for MAST and ITER, the response field is found to be greatly reduced, compared to the vacuum field produced by the RMP coils. This field reduction relies strongly on the screening effect from the toroidal plasma rotation. Numerical modeling also quantifies the 3D distortion of the plasma surface, induced by the RMP field. A correlation is found between the poloidal distribution of the computed plasma normal displacement and the observed density pump-out effect in MAST experiments. Generally the density pump-out tends to occur when the surface plasma displacement peaks near the separatrix.

1. Introduction

It is well recognized that the resonant magnetic perturbations (RMP), produced by specifically designed magnetic coils, can significantly modify the plasma ELM behaviour [1-3]. The non-resonant and resonant field harmonics from these RMP coils can also provide a toroidal torque changing the plasma flow. A realistic modeling of these effects should include the response of the plasma to the RMP fields, in addition to the vacuum field produced by the coils. So far most of the plasma response modeling has been performed assuming reduced MHD models, and/or in simplified geometry (cylindrical plasma or toroidal plasma with only edge regions) [4-5]. Most of the previous work tries to understand the non-linear interaction between the plasma response and the rotation braking (the RMP field penetration dynamics) [4-6]. In this work, we model the *linear* response of the plasma to the RMP fields, using the MARS-F/K codes [7-8]. The linear MHD code MARS-F, and its drift-kinetic hybrid extension MARS-K, solve full ideal/resistive MHD equations in full toroidal geometry including the vacuum regions, the outer conducting structures, and the RMP coils. This allows us to study the *steady-state* response of the plasma to external fields, at *given* plasma rotation. The RMP response of ELMy H-mode plasmas for MAST and ITER has been modeled.

2. Modeling tools

MARS-F/K solves the single-fluid, perturbed MHD equations in full toroidal geometry. For the purpose of the RMP response modeling, the vacuum field equations outside the plasma, the thin resistive wall equation (when applicable), and the coil equations (Ampere's law) are solved together with the MHD equations for the plasma. A resistive-inertial plasma model, with arbitrary toroidal flow and flow shear, is assumed. We consider both the bulk thermal ion flow and the electron flow. The latter consists of the *ExB* fluid flow and the electron diamagnetic flow. In the present study, the effect of the electron flow is crudely modeled by simply replacing the ion flow by the electron one in the equation for Ohm's law, yet staying in the single-fluid approximation. The RMP field response modeling requires solving a linear antenna problem, where the source term is specified as the current flowing in the RMP coils.

Since this is a linear problem, for axi-symmetric equilibria, we only need to consider a single toroidal mode number n at one time. Therefore, the source current is assumed to have an $exp(in\varphi)$-depedence along the toroidal angle φ.

3. Modeling results for MAST plasmas

We have carried out extensive modeling of the RMP experiments in MAST. Figure 1 shows one example, based on an equilibrium from the discharge 20333 at 250ms. This discharge has 700kA plasma current, with the toroidal vacuum field of 0.49T at the major radius of 0.83m. As in experiments, we focus on studying the plasma response to the $n=3$ RMP field, produced by a pair of internal coil sets, located above and below the outboard mid-plane of the torus. The currents in the upper and lower sets of coils can flow in the same direction (even parity) or in the opposite direction (odd parity). Shot 20333 is in H-mode operation, with the edge pedestal region covering $0.94<\psi_p<1$, as shown by the radial profile of the plasma density, measured by the Thomson scattering system (Fig. 1(b)). ψ_p here denotes the normalized equilibrium poloidal flux. The normalized beta value for this plasma is 2.86, far below the MARS-F computed no-wall limit of 4.24, for the $n=3$ ideal external kink mode.

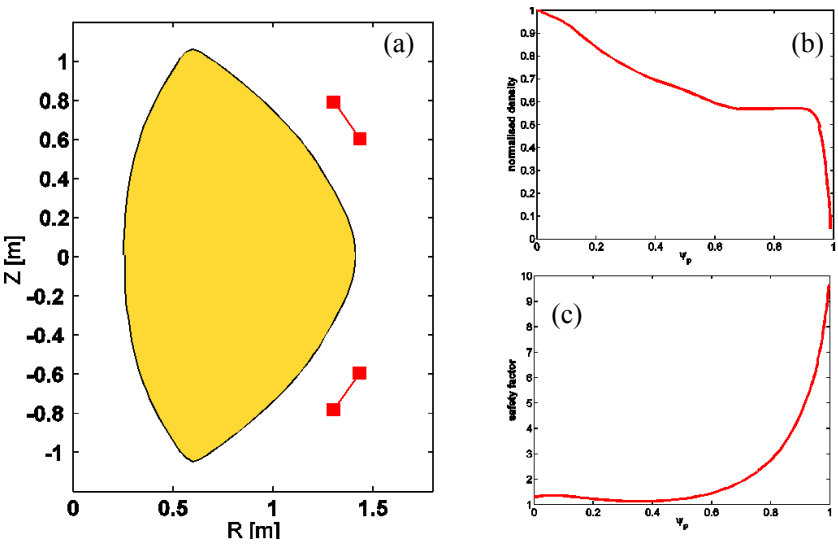

FIG.1. Equilibrium configuration for RMP modeling of MAST shot 20333: (a) the plasma boundary shape and the RMP coil geometry, (b) the normalized equilibrium density profile, (c) the safety factor.

We find that, as expected, the resistive plasma response near the plasma edge significantly modifies the resonant spectrum of the vacuum field, produced by the RMP coils. This is demonstrated by comparing Figs. 2(a) and (b), computed by MARS-F for the case shown in Fig. 1. The plasma resistivity here is assumed to be small, with the Lundquist number equal to 10^8 in the plasma centre, and about 10^6 in the plasma edge (the radial profile of the

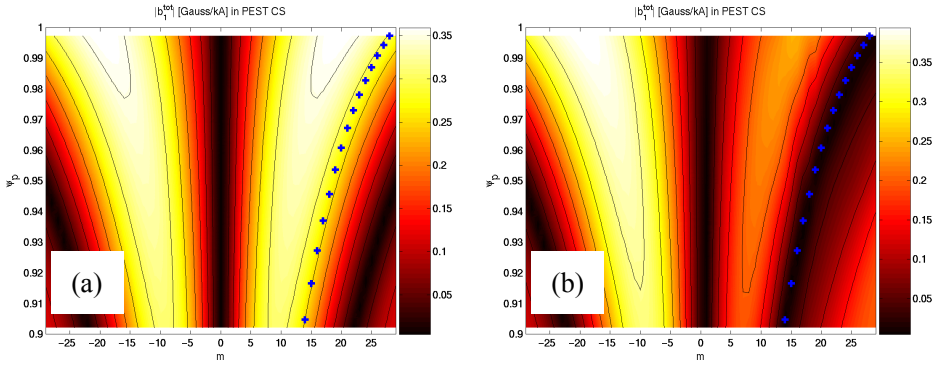

FIG.2. Comparison of the poloidal spectra near the plasma edge region, between the vacuum field and the total field including the plasma response, computed by MARS-F for shot 20333 with odd parity of the coil current. The symbols '+' indicate the location of q=m/n rational surfaces. The resonant harmonics in the pedestal region have m=18,...,28.

resistivity is assumed proportional to $T_e^{-3/2}$, where T_e is the electron temperature). The odd parity coil configuration is used. Figure 2(a) shows the poloidal components of the MARS-F computed radial vacuum field, in the PEST-like straight field line coordinate system. This vacuum field spectrum agrees quantitatively with that obtained by the Biot-Savart based-ERGOS code [9]. The resistive plasma response, however, significantly reduces the field amplitude near rational surfaces for resonant harmonics, effectively forming a deep 'valley' in right hand side of the spectrum diagram. This trend of (significant) reduction of the resonant field amplitude due to the plasma response, at rational surfaces, seems to be robust for various plasma and coil configurations, including the ITER case shown in the next Section. In fact the resistive response for this MAST case is close to the ideal plasma response, in which the resonant field amplitude vanishes exactly at the rational surface.

This reduction is mainly due to the strong shielding effect coming from the fast toroidal plasma rotation, which is about 15% of the Alfven speed in the plasma centre, as shown by Fig. 3. As a consequence, the resistive plasma response leads to a significant reduction of the Chirikov parameter [10], that is often used to characterize the magnetic field line ergodization, thought to be associated with the ELM mitigation by the RMP field. We also notice a slight field amplification effect for the $m<0$ non-resonant harmonics. This amplification normally depends on how close the plasma is to the marginal stability of ideal external kink modes. The shape of the non-resonant part of the spectrum is not much disturbed by the plasma response.

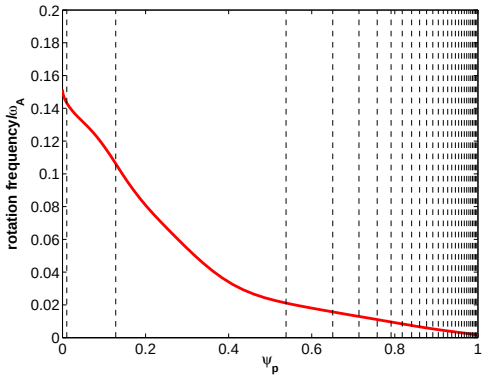

FIG.3. The toroidal plasma rotation profile for shot 20333, from the charge exchange measurements. Vertical lines indicate the radial location of rational surfaces for n=3.

Figure 4 investigates the screening effect of the toroidal plasma rotation on the RMP field. We scale the rotation amplitude, while fixing the experimental radial profile. Figure 4(a) shows the ratio of the total (i.e. the vacuum plus the pure plasma response) field amplitude to that of the vacuum field, for resonant harmonics at corresponding rational surfaces. The same plasma resistivity is assumed as in Fig.2. The field amplitude generally experiences a significant reduction, compared to the vacuum field, due to the plasma response. At fast plasma rotation, which is the experimental case, the total field can be several orders smaller than the vacuum field, in particular in the plasma core region, where the rotation speed is higher, and the plasma

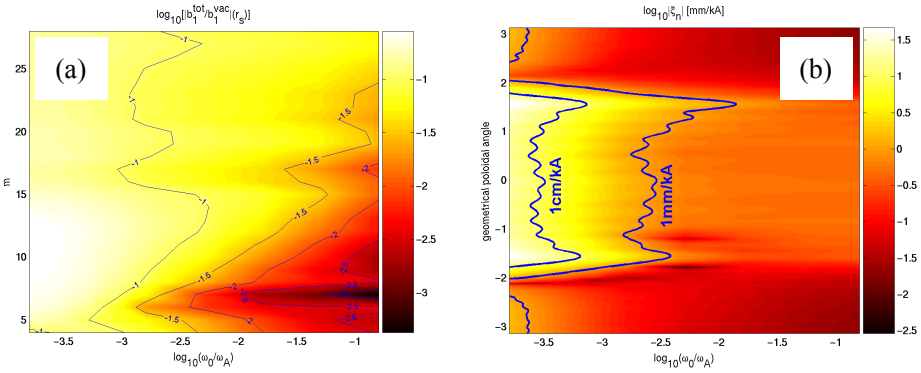

FIG.4. The effects of rotational screening of the RMP field for MAST shot 20333: (a) the computed total field amplitude, normalized by the vacuum counterpart, for the resonant poloidal harmonics, (b) the computed normal displacement along the plasma boundary surface. The experimental rotation frequency of $\omega_0=0.15\,\omega_A$ is off the RHS in the figures.

resistivity is lower. The total field amplitude increases with decreasing rotation speed, reaching about 10% of the vacuum field across all the rational surfaces, at the rotation speed of about 0.1% of the Alfven speed. In reality, the plasma toroidal rotation is often reduced by various momentum damping mechanisms, during the RMP field penetration process. This situation is modeled here in an *ad-hoc* manner, by artificially reducing the rotation speed.

The RMP field also causes a 3D distortion of the plasma surface, which potentially leads to the formation of a 3D equilibrium in the steady state. This may in turn modify the stability properties for local modes. MARS-F allows us to compute the steady state plasma displacement, but in a linear sense, with given plasma rotation. Figure 4(b) shows the normal displacement of the plasma surface with varying plasma rotation speed. The amplitude of the displacement is plotted along the geometrical poloidal angle. The contour lines show the 1cm/kA-turn and 1mm/kA-turn levels, respectively. We find a sharp increase of the plasma displacement level with decreasing rotation speed. For the MAST case considered here, MARS-F predicts mm-level of plasma displacement with the experimental rotation. However, several cm's displacement can be expected if the plasma rotation is strongly damped. The experimentally measured displacement in MAST, using EFCC, varies from 0 to a couple of cm's [11]. Finally, we notice that the plasma displacement peaks at different poloidal angle, with varying rotation. The displacement tends to peak more near the X-points as the rotation speed is reduced.

Numerically, we find a correlation between the poloidal distribution of the plasma surface displacement, and the density pump-out effect observed in MAST experiments. This is reported in Figs. 5-7. The density pump-out has been observed in both L-mode and H-mode plasmas in MAST, with both the odd and even parity RMP coil configurations. There are cases when just one parity triggers pump-out, and cases when neither parity gives an effect [2,10]. Figure 5 shows one example based on 25056, where a similar shot with the even parity configuration triggers pump-out, but another similar shot with odd parity does not produce any effect. The MARS-F computated plasma surface displacement, assuming experimental rotation, has a substantially different distribution. The odd parity configuration causes a large plasma displacement near the outboard mid-plane, whilst the even parity causes the displacement peaking near the X-points.

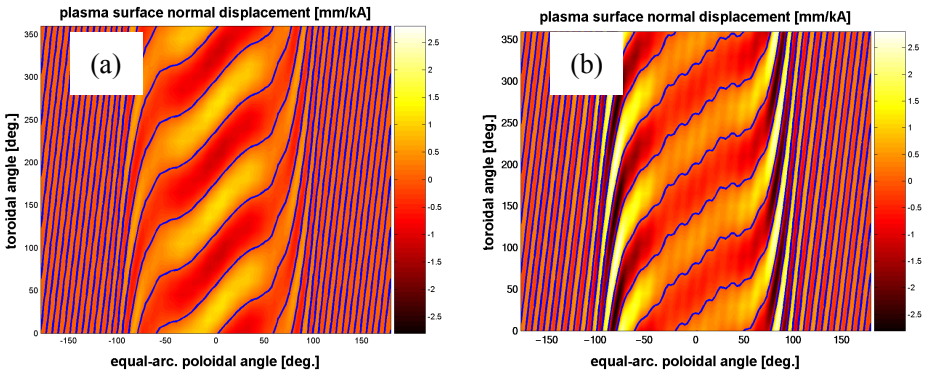

FIG.5. The RMP field triggered normal displacement of the plasma surface, plotted along the poloidal (in the equal-arc coordinate system) and the toroidal angles, with (a) odd parity and (b) even parity coils configurations. The contour lines show the zero displacement level. The displacement is computed by MARS-F for MAST shot 25056.

Figure 6(a) compares the amplitude of the surface displacement along the poloidal angle for two parities. The difference becomes even more clear when the displacement is plotted in the poloidal plane, shown by Fig. 6(b). The dashed line shows the equilibrium plasma surface. Two solid lines (the color coding coincides with Fig. 6(a)) show the exaggerated distortion of the plasma surface due to the 3D normal displacement. The displacement, in mm/kA-turn, is

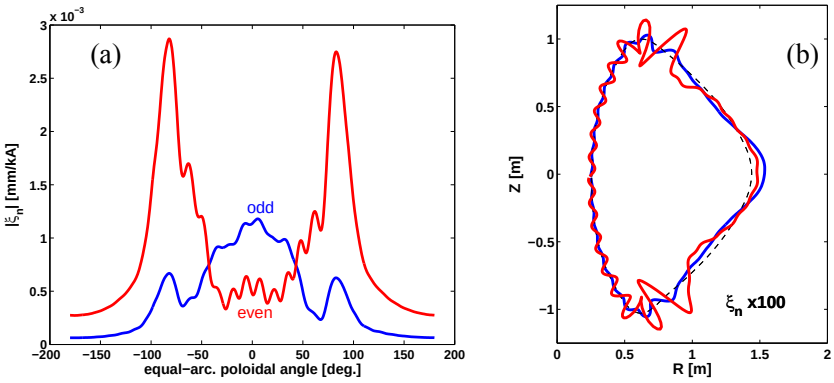

FIG.6. Comparison of the MARS-F computed normal displacements of the plasma surface with odd versus even parities of the RMP coil current, for shot 25056: (a) the amplitude of the displacement along the equal-arc poloidal angle, (b) the real part of the displacement in the R-Z plane, at the toroidal angle where the RMP coil current has zero toroidal phase.

multiplied by 100 for this plot. The even parity configuration in this case causes a large distortion of the plasma surface near the X-points, in correlation with the density pump-out effect observed in the experiment.

Our additional modeling covers all types of the MAST plasmas from the RMP experiments so far, and we find that the ratio of the displacement peaking near the separatrix, to that at the outboard mid-plane, seems to be the best indicator for the observed density pump-out effect. In particular, this indicator works perfectly well for all L-mode plasmas, as shown in Fig. 7(a), where we plot the experimental observations (1 corresponds to the pump-out effect, and 0 corresponds to non-effect) versus the MARS-F computed displacement peaking ratio. The vertical dashed line, which separates the two cases, is chosen to be about 1.4. The database includes all types of plasma and coil configurations. Both the ion and electron flow models are considered for Ohm's law. For H-mode plasmas (Fig. 7(b)), the same threshold value of about 1.4 still holds for all cases where the pump-out effect is observed. But there are two shots without the pump-out effect, for which the indicator's value is larger than 1.4. Careful examination shows that one shot (24460) is experimentally near the pump-out threshold during the q_{95} scan. Modeling results by scanning q_{95} also show marginal conditions for pump-out for this shot. The other shot (24924), for which the modeling fails to agree with

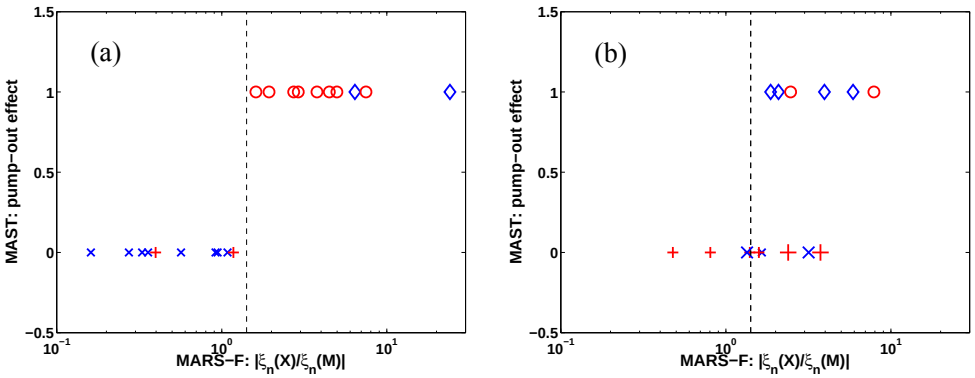

FIG.7. Correlation between the computed normal displacement of the plasma surface, and the observed density pump-out effect in experiments. Plotted is the experimental density pump-out effect (0=no effect, 1=with effect) versus the ratio of displacement peaking near the X-point ($\xi_n(X)$) to that at the outboard mid-plane ($\xi_n(M)$), for various MAST (a) L-mode and (b) H-mode plasmas . The odd parity coil configuration is denoted by '×' and '◊', even parity by '+' and '○'. Experimental rotation is used in the modeling of each plasma. The shot 24924 is denoted by symbols of larger size.

experiments, has a special, ITER-like plasma shape. Careful modeling is required to investigate the sensitivity against the equilibrium reconstruction for this shot. Unfortunately, experimental constraints so far do not allow a sensitivity study over plasma parameters, such as q_{95}, for this configuration.

Another possible figure of merit, related to the displacement ratio, is the amplitude of the last resonant harmonic (with the largest *m* number) at the plasma surface. MARS-F results show that the density pump-out occurs at a large amplitude (compared with the peak amplitude of non-resonant harmonics) but does not occur at a small amplitude. Again a perfect correlation is observed for all types of L-mode plasmas in MAST, even using the vacuum field alone. A somewhat worse correlation, compared to that of the displacement ratio indicator, is obtained for the H-mode plasmas. In this case, a slight improvement can be made by including the plasma response field in evaluating the amplitude of the last resonant harmonic.

4. Modeling results for ITER plasma

We compute the plasma RMP response for one of the latest designs of the ITER 15MA inductive H-mode scenario (under the burning condition) [12]. A recent design of the in-vessel ELM control coils is considered as shown in Fig. 8(a). We have performed the RMP computations for the toroidal mode numbers *n=1,2,3,4*. We report here the results for the *n=4* field configuration. We assume -120° (120°) toroidal phase shift between the upper (lower) coil current and the mid-plane coil current. This phase configuration seems to give the largest vacuum field amplitude at the corresponding rational surfaces for *n=4*. The radial profile of the safety factor *q* is shown in Fig. 8(b). For this plasma, the minimum *q* value is near 1, the edge *q* value is just above 4 (after slightly smoothing the plasma boundary shape near the separatrix as shown in Fig. 8(a)). The value of q_{95} is about 3.2. The peculiar *q*-shape near the plasma edge is caused by a large bootstrap current. The resonant poloidal harmonics are *m=5,...,16*. The normalized beta is about 2.1, far below the no-wall limit of about 4.4 for the *n=4* external kink mode.

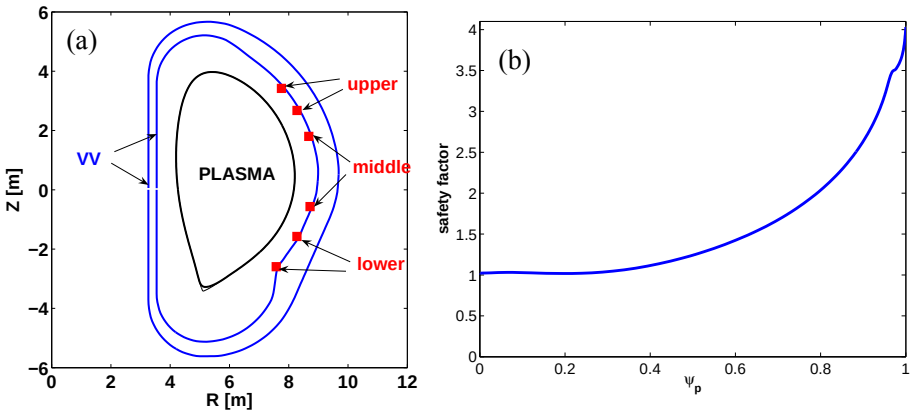

FIG.8. (a) The RMP coil configuration for the ITER 15MA ELMy H-mode scenario. Shown also are the plasma boundary shape and the shape of the ITER vacuum vessel. (b) The equilibrium profile of the safety factor.

Figure 9 summarizes the MARS-F computed results for this ITER case. We again consider the resistive plasma response, with the $T_e^{-3/2}$ resistivity model, and keeping the Lundquist number to be 10^8 in the plasma centre. We vary the plasma rotation amplitude, fixing the rotation profile to that from the ASTRA prediction [12]. Figure 9(a) shows the contour plot for the total radial field amplitude, normalized by the corresponding vacuum field, at rational surfaces for all resonant harmonics. At the expected plasma rotation speed, which is about *1.3%* of the Alfven speed in the plasma centre according to ASTRA, and corresponds to the value 0 along the x-axis in the figure, the amplitude of the total radial field at rational surfaces is 2-3 orders of

magnitude smaller than that predicted by the vacuum calculations in the plasma inner regions, and about *10%* of the vacuum field in the plasma edge region. Decelaration of the toroidal rotation increases the plasma response everywhere, in particular in the inner regions. At the rotation speed of about *0.01%* of the Alfven speed, the plasma response amplitude at rational surfaces can reach that of the vacuum level. Figure 9(b) shows the amplitude of the plasma surface displacement, along the geometrical poloidal angle as we vary the rotation speed. At the rotation speed close to the expected value, the normal displacement is about 1mm per kA-turn of the *n=4* current, in a wide range of the poloidal angle on the low-field-side. The middle set of ITER RMP coils has 9 equally distributed coils along the toroidal angle, each spanning

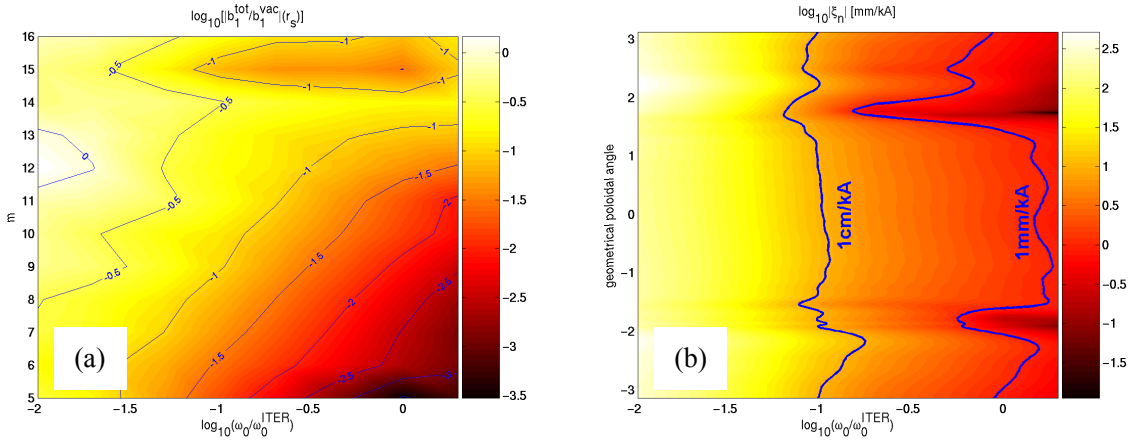

FIG.9. The effects of rotational screening of the RMP field for the ITER plasma: (a) the total field amplitude, normalized by the vacuum counterpart, for the resonant poloidal harmonics, (b) the computed normal displacement along the plasma boundary surface.

20^o and carrying 96kAt maximal current. This corresponds to about 30kAt of the n=4 current (assuming a toroidal phasing of +-+-+-+-±), which can cause about 3cm plasma surface displacement at the predicted ITER rotation. The displacement increases rapidly with decreasing rotation speed. In reality, the plasma rotation will likely be reduced during the field penetration process. Therefore the plasma response, predicted for the rotation speed below the expected value in ITER, can also be of practical significance.

5. Conclusion and discussion

The linear, full toroidal modeling of the plasma RMP response for MAST and ITER plasmas, by the MARS-F code, leads to the following key observations:

- With reasonable assumptions on the plasma resistivity and toroidal rotation, the plasma response tends to reduce the amplitude of resonant harmonics at the corresponding rational surfaces, compared to the vacuum RMP field. This reduction can exceed one order of magnitude even in the plasma edge region, where the resistivity is high and the rotation is slow. Consequently, the vacuum RMP model may significantly over-estimate the field line ergodization.

- Sufficiently fast toroidal plasma rotation has strong screening effects on the RMP field. The RMP induced 3D distortion of the plasma boundary surface is also enhanced with decreasing rotation speed. This dependence is quantified for both MAST and ITER plasmas.

- A good correlation is found between the poloidal distribution of the computed plasma surface normal displacement, and the observed density pump-out effect in MAST experiments. A threshold value of about 1.4 is found, for the ratio of the displacement peaking near the X-point to that at the outboard mid-plane. This figure of merit seems to work perfectly well for all types of MAST L-mode discharges carried out so far. In other words, the density pump-out effect tends to occur, when the surface plasma displacement peaks near the X-point. Thorough investigations are needed to understand this correlation.

We point out two important limitations associated with the MARS-F computations. (i) The RMP field penetration dynamics through the plasma, which involves non-linear coupling of the plasma field response to the momentum damping, is not self-consistently modeled. The results presented here are directly applicable to experiments only in a perturbative sense (i.e. with *ad-hoc* changing of plasma rotation). This is the case for most of the MAST pulses presented here. The linear results can be more rigorous for experimental situations where the RMP field does not cause a significant braking of the plasma rotation. (ii) We considered so far only the screening effect of the toroidal plasma rotation. In reality, the poloidal rotation (in particular from the electron diamagnetic rotation in the pedestal region of H-mode plasmas) may also play a significant role for the field shielding [13-14].

Finally, we notice that the ELMs are systematically mitigated in present machines, despite the rotational shielding effect for the resonant harmonics. This is either because of the loss of the screening effect due to the rotation damping, or, in case of no rotation damping during the RMP experiments, because of mitigation mechanisms beyond the present field line stochastization theory.

In order to study the transient plasma response and rotation braking, the nonlinear code BOUT++ [15] will be used in the future, in order to simulate reduced ideal and resistive MHD in idealized equilibria. The linear version of BOUT++ will also be benchmarked with MARS-F.

Acknowledgements

This work was funded by the RCUK Energy Programme under grant EP/G003955 and the European Communities under the contract of Association between EURATOM and CCFE. The views and opinions expressed herein do not necessarily reflect those of the European Commission.

Reference

[1] Evans T.E. *et al*, 2006 *Nat. Phys*. **2** 419
[2] Liang Y. *et al*, 2007 *Phys. Rev. Lett*. **98** 265004
[3] Kirk A. *et al*, 2009 *Plasma Phys. Control. Fusion* **51** 065016
[4] Nardon E. *et al*, 2009 *Plasma Phys. Control. Fusion* **51** 124010
[5] Becoulet M. *et al*, 2009 *Nucl. Fusion* **49** 085011
[6] Strauss H.R. *et al*, 2009 *Nucl. Fusion* **49** 055025
[7] Liu Y.Q. *et al*, 2000 *Phys. Plasmas* **7** 3681
[8] Liu Y.Q. *et al,* 2008 *Phys. Plasmas* **15** 112503
[9] Nardon E. *et al*, 2007 *J. Nucl. Mater*. **363-365** 1071
[10] Kirk A. *et al*, "Magnetic perturbation experiments on MAST using internal coils", Paper EXD/8-2, *Proc. 23rd IAEA Fusion Energy Conference 2010*, Daejeon Korea
[11] Chapman I, *et al*, 2007 *Nucl. Fusion* **47** L36
[12] Casper T. and Polevoi A., *ITER documentation* number 2V2XYR
[13] Heyn M.F. *et al,* 2008 *Nucl. Fusion* **48** 024005
[14] Nardon E. *et al,* 2010 *Nucl. Fusion* **50** 034002
[15] Dudson B.D. *et. al*, 2009 *Comp. Phys. Comm*. **180** 1467